C-supported WO_x-Ru based Catalysts for the Selective Hydrogenolysis of Glycerol to 1,2-Propanediol

Received 00th January 20xx,
Accepted 00th January 20xx

DOI: 10.1039/x0xx00000x

Alessandro Bellè,[a] Kohei Kusada, [a, b] Hiroshi Kitagawa,[b] Alvise Perosa,[a] Lidia Castoldi,[c] D. Polidoro,[a] and Maurizio Selva, *[a]

Abstract. New C-supported bimetallic Ru-WO_x catalysts, prepared by co-impregnation of $RuCl_3$ and Na_2WO_4, proved highly efficient for the liquid-phase hydrogenolysis of aq. glycerol into 1,2-propanediol (1,2-PDO). The tuning of the catalysts composition and major reaction parameters, specifically operating at 150 °C, 5 bar of H_2, and Ru:W=4:1 mol/mol, allowed conversion of glycerol and 1,2-PDO selectivity of 73->99% and 88-98%, respectively, with a carbon loss < 5%. Ru-WO_x/C offered a steady performance for up to 7 subsequent recycles during which leaching of Ru was negligible while loss of W decreased from an initial 5 wt% (1st run) to 0.1 wt% after 5 runs. The catalysts characterization, particularly EDX analysis and high-resolution TEM images, confirmed a uniform dispersion of Ru and W on the C-surface with the presence of small Ru-nanoparticles (below 2 nm) and randomly aggregated dots which could be ascribed to WO_x clusters of size below 100 nm. Based on both Bronsted and Lewis acidity of WO_x species, a reaction mechanism was proposed through an initial dehydration of glycerol followed by a Ru-catalysed hydrogenation process.

Introduction

The majority of glycerol available in the current market, also called native glycerol, comes from renewable sources.[1] Thanks to its non-toxicity, physico-chemical properties and flexible reactivity, native glycerol is one of the top bio-based platform chemicals with literally hundreds of applications and dozens of review articles published every year on its chemical and biological upgrading. [2,3] Among the most attractive reactions, the catalytic hydrogenolysis of glycerol plays a preeminent role for the synthesis of high added-value commodity chemicals as 1,2-propanediols (both 1,2- and 1,3-propanediol isomers: 1,2- and 1,3-PDO) which are excellent solvents, intermediates, and monomers. [4,5]

This subject, with particular reference to 1,2-PDO, has been exhaustively reviewed in recent papers where the most used catalysts based on noble and other transition metals have been described focusing on the critical issue of the process, *i.e.,* the diol selectivity. [6,7,8] Scheme 1 highlights the three pathways (1-3) of dehydration–hydrogenation, dehydrogenation–dehydration–hydrogenation, and direct hydrogenolysis which are generally accepted for the conversion of glycerol to both 1,2- and 1,3-PDO, along with some major side reactions (in red) including further dehydration–hydrogenation and C-O/C-C bond cleavage processes which bring about the formation of a range of liquid derivatives (primary and sec-alcohols) and gaseous products (mostly CO, and CH_4).

Typical catalysts for the hydrogenolysis of glycerol are therefore heterogeneous bifunctional systems comprised of a metal or multimetallic component acting as an oxidation–reduction functionality for the activation of hydrogen, and an acidic or basic support providing reactive sites for the removal of hydroxyl groups (dehydration processes). The benchmark system was copper-chromite ($Cu_2Cr_2O_5$) by which 1,2-propanediol was obtained in yields >70% under comparatively mild conditions (200 °C, 14 bar H_2). [9] Notwithstanding the good results, the presence of the highly toxic chromium posed environmental and safety concerns. A variety of alternatives have been proposed using Cu-, Ni- and Co-based catalysts or even their bimetallic combinations, supported on several solids including SiO_2, MgO, ZnO, Al_2O_3, and others. [6,7,10] These studies often reported a satisfactory 1,2-PDO selectivity (85-90%), but in a range of moderate (glycerol) conversions not exceeding 70%. If the hydrogenolysis proceeded further, the onset of side-reactions of Scheme 1 made the formation of the diol drop considerably, even far below 70%. Almost quantitative conversion (90-100%) and high selectivity (91-97%) were described only in a very limited number of papers: most relevant examples included the use of a $CuAl_2O_4$ spinel,[11] $Cu/B_2O_3/SiO_2$, [12] Cu/ZnO, [13] Cu/MgO,[14] and Cu-Mg/SiO_2 [15] as catalysts.

Noble metals have been also extensively investigated for the hydrogenolysis of glycerol. Due to the vastness of this topic, the discussion is here limited to the representative cases of Pt and Ru. The comparison of Pt-based bifunctional catalysts prepared by a variety of acid or basic supports demonstrated that one of the most performant systems was achieved by using Pt on Mg/Al basic hydrotalcites: [7,16] at 220 °C and 30 bar of H_2, the conversion of glycerol was 92% and the 1,2-PDO selectivity was 93% after 20 h. The dehydrogenation–

[a] Department of Molecular Sciences and Nanosystems, Scientific Campus, Ca' Foscari University of Venice, Via Torino, 155 – Venezia Mestre, Italy; selva@unive.it
[b] Graduate School of Science, Kyoto University Yoshida-honmachi, Sakyo-ku, Kyoto, 606-8501, Japan.
[c] Department of Energy, Milan Polytechnic, Campus Bovisa - Via Lambruschini, 4a - 20156 Milano

Electronic Supplementary Information (ESI) available: Figure S1-S13 and Schemes S1-S2. See DOI: 10.1039/x0xx00000x

dehydration–hydrogenation route (path 2 in Scheme 3) was plausibly followed in this case. More recently, however, a conceptually different catalyst design allowed to obtain a Pt-In alloy which offered even better results (conversion and selectivity >99% and 91% respectively, at 200 °C, 20 bar, and 24 h). [17] Authors proposed that the Pt sites at the Pt-In alloy interface served as intrinsic catalytic centers for the activation and cleavage of C-H bonds and hydroxyl groups, while (other) discrete Pt sites suppressed the undesired C-C bond cleavage.

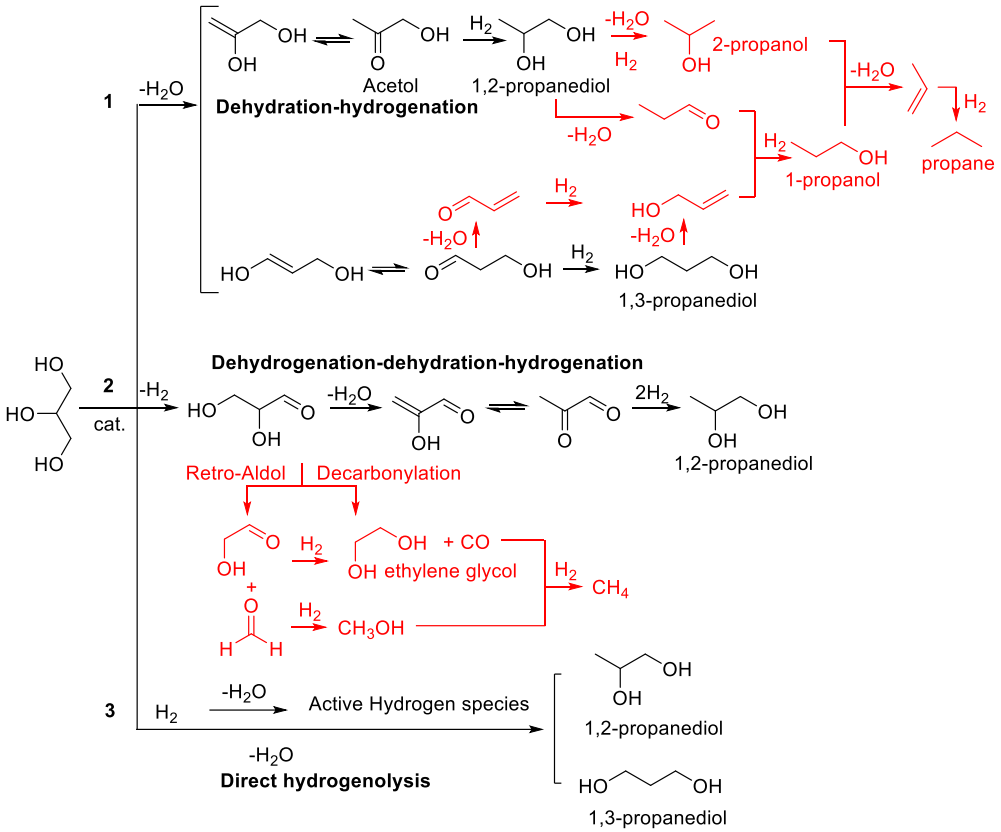

Scheme 1. Major pathways (1-3) for the hydrogenolysis of glycerol to 1,2- and 1,3-PDO, including the formation of light liquids and gaseous side-products (red insets

With respect to Pt- (and even Re- or Rh-) based catalysts, Ru-based systems usually display a higher activity for the conversion of glycerol, meaning that the hydrogenolysis may be run under comparatively milder reaction conditions; [18] though, Ru is also efficient in the C–C bond breaking. Studies have clearly highlighted how the reaction is not only affected by the metal/support combination, but also by the metal precursors and the reduction conditions.[19,20] Several strategies have been aimed to improve the formation of 1,2-PDO over Ru catalysts by increasing the density of acid groups or alternatively, the basic features of the support. Examples include the combination of Ru/AC (activated carbon) and a solid organic resin as Amberlyst 70 as an acid co-catalyst, [21] and by impregnating $RuCl_3$ on basic oxides as CeO_2 and $Mg(OH)_2$: [17,22] at 120-180 °C, 50-80 bar, and 10 h, the glycerol conversion ranged between 50 and 85%, but the 1,2-PDO selectivity did not exceed 70%. Better results however, have been achieved with bimetallic systems where a second metal component (i.e. Cu, Re) was used to restrain the cleavage of C–C bonds. [6,23] To date, most performant catalysts were obtained by co-dispersing Ru and Cu (in 3-10:1 ratio), on bentonite or zirconia as supports: at 180-230 °C and 80-100 bar, a quantitative conversion was reached with yield/selectivity of 1,2-PDO up to 85%.[24,25]

In this lively context, as a part of our research interest on the Ru/C-catalysed processes for the valorisation of bio-based compounds,[26] we were prompted to design multifunctional catalysts comprised of a binary mixture of Ru and a solid acid as WOx bearing strong Bronsted acid sites,[27] dispersed on C, indicated as Ru-WO_x/C. WO_x has been widely described as a support for Pt in the hydrogenolysis of glycerol to 1,3-propanediol,[28] but Ru-WO_x systems have been much less investigated. To the best of our knowledge, only three pertinent examples (a-b) have been reported so far (Scheme 2). [29,30,31]

In the first two cases, the reaction of cellulose and glycerol were catalysed by a mechanical mixture of Ru/C and WO_3/C or a 1% Ru supported on WO_3, respectively: the corresponding 1,2-PDO selectivity was 38% and 23% (paths a and b). The third, very recent study claimed that the conversion of fructose to 1,2-PDO was achieved on a Ru-WO_x system supported on hydroxyapatite (HAP; path c); albeit the product was obtained in a remarkably high yield (91% by GC), issues with enzymes necessary for synthesizing fructose (from

isomerization of glucose) made the latter a less convenient substrate than glycerol to produce 1,2-PDO. [32]

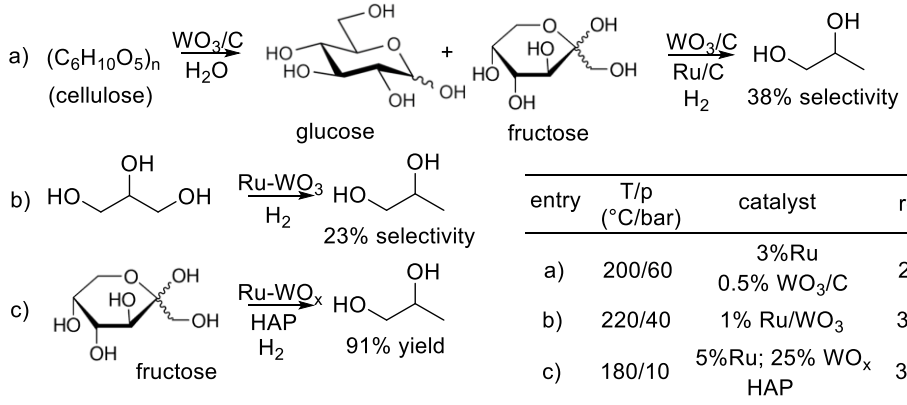

entry	T/p (°C/bar)	catalyst	ref
a)	200/60	3%Ru 0.5% WO_3/C	29
b)	220/40	1% Ru/WO_3	30
c)	180/10	5%Ru; 25% WO_x HAP	31

Scheme 2. Ru-WO_x systems in the production of 1,2-PDO

In this paper, we wish to report that by co-impregnating simple commercial precursors as $RuCl_3$ and Na_2WO_4 on carbon, a series of Ru-WO_x/C catalysts was prepared exhibiting excellent performance for the selective hydrogenolysis of glycerol. Particularly, at 170 °C and 50 bar, a sample obtained with a Ru:W molar ratio of 4 (5% Ru), allowed a conversion >99% and a 1,2-PDO selectivity of 92%, and it proved recyclable for at least, seven subsequent reactions without any loss of activity. Albeit the characterization of Ru-WO_x/C systems was challenging, analyses indicated the no metal alloy was obtained, but a strong Ru/W interaction was more than plausible due to close co-presence of very small Ru-nanoparticles (below 2 nm) highly dispersed on C, and aggregates randomly distributed on the same support, ascribed to WO_x clusters below 100 nm.

Results and Discussion

The catalysts. 5% Ru/C is described in the literature as a reference catalyst for the reduction of glycerol,[33] and it is among the preferred commercially available systems to carry out hydrogenation/hydrogenolysis of biobased compounds in water solutions.[34] For these reasons, in this paper, four bimetallic Ru-WO_x catalysts supported on C, were prepared with a constant Ru loading of 5 wt%, and a variable W content. The latter was changed sample by sample, to achieve a Ru:W molar ratio in the range of 1-16. The metal oxide was indicated as WO_x due to the co-existence of different oxidized phases of W, as described later in the characterization section. These solids were synthesized through the adjustment of co-impregnation-precipitation methods reported in the literature for the synthesis of Ru nanoparticles decorating WO_3,[35] and Pt-Ru-Sn-W/C.[36] $RuCl_3 \cdot H_2O$ and Na_2WO_4 were used as the metal precursors and a commercial powdered carbon (NORIT SX 1G) was the support. The properties of such C-support were described by us in a previous paper.[24] In a typical synthesis, a suspension of carbon (NORIT SX 1G), $RuCl_3 \cdot H_2O$, Na_2WO_4, and water was stirred at rt, added with conc.d aq. HCl, and heated at 80 °C. After the removal of water, the solid was dried, reduced with H_2 (25 mL/min, 300 °C, 3 h), washed with milli-Q water, and filtered. It was then dried again and stored. The samples achieved by this procedure had a nominal metal loading of 5wt% for Ru, and of 9, 2, 1 and 0.5 wt% for W, respectively. They were labelled according to the different W content, as Ru-9WO_x/C, Ru-2WO_x/C, Ru-1WO_x/C, and Ru-0.5WO_x/C.

Two other bimetallic catalysts were prepared by a different approach. Following the impregnation method described above, Na_2WO_4 was first dispersed on carbon powder (NORIT SX 1G) to obtain a nominal W loading of 2 wt%. The sample was labelled as 2WO_x/C and it was used as a support to introduce the second metal component, Ru, either through a subsequent impregnation or via a mechanical mixing. In the first case (impregnation), a suspension of $RuCl_3 \cdot H_2O$ and 2WO_x/C in water was stirred at rt, added with conc.d aq. HCl, and heated at 80 °C. The solid was then dried, reduced and washed through the protocol used above for co-impregnated catalysts. This sample was labelled as [Ru-2WO_x/C]$_{ts}$ (ts=two-step synthesis): the corresponding metal loadings were 5 and 2 wt% for Ru and W, respectively. In the second case (mechanical mixing), the catalyst was obtained by mixing 2WO_x/C (150 mg) and commercial 5% Ru/C (150 mg). The sample was labelled as [Ru-2WO_x/C]$_{mm}$ (mm=mechanical mixture) with metal loadings of 2.5 and 1 wt% for Ru and W, respectively.

Further details on the catalyst synthesis are described in the ESI section.

After the preparation, an aliquot (50 mg) of each solid was dissolved under strong acid/oxidizing conditions in the presence of aqua regia (5 mL) and H_2O_2 (1 mL), under MW irradiation, and the recovered aqueous solutions were subjected to ICP/MS analyses (other details are given in the experimental section). Results are summarized in Table 1.

Table 1. Metal loadings of Ru and W in the prepared samples

Entry	Sample label	Synthetic method	Ru (wt%)[a]		W (wt%) [a]		Ru:W (molar ratio)
			N	D	N	D	
1	Ru-0.5WO_x/C	Co-impregnation	5	4.8	0.5	0.4	16:1
2	Ru-1WO_x/C	Co-impregnation	5	4.7	1	1	8:1
3	Ru-2WO_x/C	Co-impregnation	5	4.8	2	2	4:1
4	Ru-9WO_x/C	Co-impregnation	5	4.5	9	6	1.3:1
5	2WO_x/C	Impregnation	-	-	2	2	-
6	[Ru-2WO_x/C]$_{ts}$	Two-steps impregnation	5	4.8	2	2.1	4:1
7	[Ru-2WO_x/C]$_{mm}$	Mechanical mixing	2.5	Nd[b]	1	Nd[b]	4:1

[a] Metal (Ru or W) loading of the catalyst as wt%; N: nominal loading from the preparation; D: loading determined by ICP measures. [b]Nd: not determined.

For three out of the four solids obtained by the co-impregnation procedure, specifically for Ru-2WO_x/C, Ru-1WO_x/C and Ru-0.5WO_x/C, the metal loading (Ru or W; wt%) determined by ICP analyses (D values) matched the nominal metal content (N values) expected from the amounts of $RuCl_3 \cdot H_2O$ and Na_2WO_4 used during the synthesis (entries 1-3). From the same (ICP) analyses, the residual Na was measured in each sample: the corresponding quantity (≤0.1%) equalled that of the commercial 5% Ru/C.

A deviation was instead observed for the sample Ru-9WO_x/C where the measured loadings of metals, especially for W, were lower than expected (entry 4). The Ru:W molar ratio was of 1.3 rather than 1. Moreover, a remarkably high Na quantity (5 wt%) was detected. Attempts to repeat the preparation of this catalyst gave unsatisfactory and not reproducible results which led us to conclude that the synthetic protocol was not suitable to make materials with W-loading exceeding 2 wt%. High relative amounts of metal precursors plausibly interfered with each other in the co-adsorption on the C-support making their dispersion not effective. Whichever the reason, the Ru-9WO_x/C system was abandoned.

ICP analyses of other samples obtained by single or two-step impregnation as 2WO_x/C and [Ru-2WO_x/C]$_{ts}$ gave a good correspondence between nominal and actual metal content for both Ru and W (entries 5 and 6).

The catalytic activity of Ru-WOx/C systems. The performance of Ru-WO_x/C systems was investigated for the hydrogenolysis of aqueous glycerol. Due to the complexity of the reaction and the vast body of literature available, a preliminary screening was conducted using a commercial 5% Ru/C sourced by Aldrich, under the conditions more often reported for the process, particularly T and p in the range of 100-200 °C and 40-80 bar of H_2, respectively (see ESI section, Figures S1 and S2).[37,38,39] In light of these results and other findings on the effect of the H_2 pressure,[40] experiments were initially performed at 150 °C and 5 bar of H_2 for 6 h, in a stainless-steel autoclave charged with an aqueous solution of glycerol (5 mL, 5 wt%) and the chosen catalyst (150 mg).

The reaction provided both liquid and gaseous products (cf. Scheme 1). The attention was focused on liquid derivatives including 1,2-PDO, EG (ethylene glycol), and lighter alcohols (1- and 2-propanol, ethanol and methanol). The formation of these compounds and the conversion of glycerol were determined by GC, using triglyme as an external standard, and their structure confirmed by GC/MS through comparison with authentic commercial compounds. Other products, named as "others", included gases (mostly CO, CO_2, and CH_4) whose total amount was the complement to 100 of the overall reaction selectivity. The carbon loss in the liquid phase (% C_{loss}) was evaluated from the carbon balance (%$C_{balance}$), as the difference of initial moles of glycerol and the total molar amount of all liquid products.

$$\%C_{Balance} = \frac{\sum moles\ of\ products\ in\ the\ liquid\ phase - initial\ moles\ of\ glycerol}{initial\ moles\ of\ glycerol} * 100$$

$$\%C_{loss\ in\ the\ liquid\ phase} = 100 - \%C_{Balance}$$

Results are reported in Table 2. The table also includes tests with the commercial 5% Ru/C catalyst and 2WO_x/C.

The commercial Ru/C catalyst allowed a 60% conversion, but it clearly favoured the multiple hydrogenolysis of glycerol: EG (80%) was the major liquid product formed along with a sizeable amount of gaseous derivatives. A high carbon loss of 51% was determined (entry 1). By contrast, a striking improvement in the reaction selectivity and carbon balance was manifest when co-impregnated WO_x-modified Ru/C systems were used. All such catalysts provided the almost exclusive formation of 1,2-PDO (97-98%) and displayed negligible C-C bond cleavage producing only traces (≤3%) of liquid by-products (entries 2-4). Another salient aspect was the effect of the amount of WO_x: glycerol conversion showed a progressive increase from 40% to 61% and 73%, when lowering the Ru:W molar ratio from 16:1 to 8:1 and 4:1.

Table 2. The comparative performance of mono- and bi-metallic catalysts, Ru/C, WO_x/C and Ru-WO_x/C, in the hydrogenolysis of glycerol at 150 °C and 5 bar (H_2), for 6 hours.

Entry	Catalyst	Conv. (%)	Liquid products (Selectivity, %)					C_{loss} (%)
			1,2-PDO	EG	1-PrOH	2-PrOH	MeOH + EtOH	
1	Ru/C	60	13	80	-	-	7	51
2	Ru-0.5WO_x/C	40	98	0.5	1	0.5	1	5
3	Ru-1WO_x/C	61	98	0.5	0.5	1	1	2
4	Ru-2WO_x/C	73	97	0.5	0.5	1	1	3
5	[Ru-2WO_x/C]$_{ts}$	35	96	1	0.5	0.5	1	5
6	[Ru-2WO_x/C]$_{mm}$	15	97	1	1	0.5	0.5	5
7	2WO_x/C	0						

All reactions were carried out using an aqueous solution of glycerol (5 mL, 5 wt%) and the chosen catalyst (150 mg).

On balance, the best performing system was Ru-2WO_x/C (Ru:W=4 mol/mol) by which the highest conversion (73%) was reached with high 97% selectivity towards 1,2-PDO (entry 4). Other experiments in Table 2 further corroborated this observation: 2WO_x/C was totally ineffective for the reaction (entry 7), while both [Ru-2WO_x/C]$_{ts}$ and [Ru-2WO_x/C]$_{mm}$ allowed a high 1,2-PDO selectivity (96%) with low carbon loss (≤5%), although the corresponding glycerol conversion was only 35% and 15%, respectively (entries 5 and 6). This led to conclude that W-oxide was not involved in the catalysis, but its contribution was crucial to limit C-C bond cleavage by Ru. Moreover, interactions between the metal catalyst components were optimized when the metal precursors were simultaneously impregnated on the C-support. Multiple effects improving both the glycerol conversion and the products distribution could be anticipated from the literature, including the formation of: i) WO_x clusters on the carbon surface providing Brønsted acid sites;[41] ii) small metal particles originated from an acid chloride precursor of Ru.[19]

Based on these results, the study was continued using the best system identified in Table 2: Ru-2WOx/C (Ru:W 4:1 molar ratio). The influence of temperature and pressure as major reaction parameters was investigated in more detail.

Effects of T and p. The hydrogenolysis of glycerol catalysed by Ru-2WO_x/C, was explored at different T and p in the range of 120-170 °C and 5-35 bar of H_2, respectively. Other conditions were kept unchanged with respect to Table 2 [aq. glycerol solution: 5 mL, 5 wt%; t = 6 h; catalyst: 150 mg). Results are reported in Figure 1.

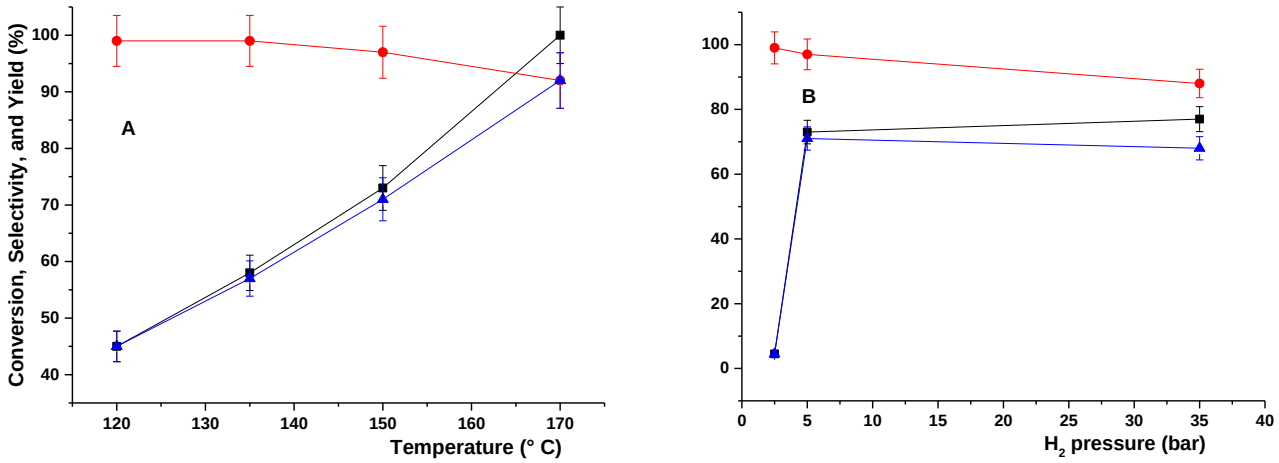

Figure 1. Influence of the temperature (A, p=5 bar) and pressure (B, T=150 °C) on the conversion (-■-) of glycerol, and the selectivity (-●-) and yield (-▲-) towards 1,2-PDO. Other conditions: aq. glycerol= 5 mL, 5 wt%, Ru-2WO_x/C=150 mg; 6 h.

At a constant pressure of 5 bar (Figure 1A), increasing the temperature allowed a quantitative conversion of glycerol (black profile) and improved the yield of 1,2-PDO from 45 to >92% (blue profile); while, the corresponding selectivity (red profile) remained substantially steady and above 97% at 120-150 °C, with a slight drop to 92% at 170 °C due to the formation of ethylene glycol (EG: 2%) and light alcohols (MeOH, EtOH and propanols: 6% in total) as by-products. In all cases, the carbon loss was negligible (≤5%).

At a constant temperature of 150 °C (Figure 1B), a sharp increase of both the glycerol conversion and the yield of 1,2-PDO from 3 to 73% and 3 to 71%, respectively, was noticed when the pressure was raised from 2 to 5 bar. This was consistent with the availability of gaseous H_2 in the reactant solution: at 50 °C for example, the H_2 solubility in water has been reported to increase almost linearly with pressure from 1 to 5 bar.[42] Minimal, if any, effects were observed on the 1,2-PDO selectivity (97-99%). A further rise of the pressure up to 35 bar had limited consequences on the conversion, but it reduced the selectivity and the yield to 88% and 68%, respectively, in favour of EG (1%) and light alcohols (11% in total). The further increase of the H_2 solubility in water which triplicates in the interval 5-35 bar, [43] plausibly accounted for an improved activity of the catalyst towards C-C bond cleavage reactions. Similar effects of the H_2 pressure were described for the hydrogenolysis of glycerol in the presence of both Cu- and

Ru-based systems.[44,45] Moreover, for the same reaction catalyzed by Ru/CsPW [Ru-doped acidic heteropoly salt, $Cs_{2.5}H_{0.5}[PW_{12}O_{40}]$ (CsPW)], over-reduction of W(VI) was reported at pressure >10 bar, resulting in a decrease of the catalyst acidity and a poorer performance.[39]

Additional experiments demonstrated that even at 150 °C and 5 bar (conditions of Figure 1, left), by prolonging the hydrogenolysis for up to 12 hours, a quantitative conversion of glycerol was achieved with a 1,2-PDO selectivity of 87% (other liquid by-products were EG and light alcohols) and a carbon loss below 5%. This result demonstrated that the WO_x-modified Ru catalyst allowed an outcome comparable to the best existing methods for the synthesis of 1,2-PDO from glycerol (based on Ru/Cu-based systems[23,24]), with the advantage of requiring far milder reaction conditions (150 °C and 5 bar vs 180-230 °C and 80-100 bar).

Finally, the effect of glycerol concentration was explored using 5-20 wt% aqueous solutions at 150 °C and 5 bar. This study showed a five-fold drop of the conversion, from quantitative to ca 20%, with the more concentration solution (20 wt%), while 1,2-PDO selectivity increased from 88% to >95%. Overall, the extent of undesired C-C cleavage reactions and dehydration/ hydrogenation of 1,2-PDO (paths 1 and 2, Scheme 1) could be tuned below 5% also by the concentration effect, providing that the conversion did not exceed 50% (Details of this investigation are described in the ESI section, Figure S3).

Recycle of the catalyst. The catalyst in a liquid-phase reaction may affect up to one third of the total cost of the process meaning that its recovery and reuse are fundamental to the economic and environmental sustainability of any catalytic protocol.[46] With the aim of exploring this aspect, recycle experiments were carried out using the reference catalyst, Ru-$2WO_x$/C, under conditions chosen to control the reaction outcome at a final conversion not exceeding 75%. Hydrogenolysis tests were therefore performed for 6 hours at 150 °C and 5 bar of H_2, in the presence of Ru-$2WO_x$/C (150 mg) and an aq. solution of glycerol (5 mL, 5 wt%) (conditions of Figure 1, left). Once a (first) reaction cycle was complete, the catalyst was filtered, washed with water (15 mL), dried overnight under vacuum (70 °C at 5 mbar), and recycled for a second hydrogenolysis run. The overall sequence was repeated for 7 subsequent experiments. Of note, the mass loss of dried catalyst was on average 0.01% from one recycle to another (with respect to the initial sample, the weight of the residual catalyst after the 7th test was 140 mg). Results are reported in Figure 2. The catalytic performance of Ru-$2WO_x$/C was unaltered over 7 subsequent recycles: both the conversion (black profile) and the 1,2-PDO selectivity (green bars) were substantially steady at about 70% and >95%, respectively, with changes within the experimental error (≤5%). However, ICP analyses of aq. solutions from 1st, 2nd and 5th recycles proved that the chemical composition of the catalyst changed: leaching of Ru was always negligible (<0.01 wt%), but a significant loss of W (ca 5 wt%) occurred after the first reaction and then it quickly decreased to 0.3 wt% and tended to stabilize at 0.1 wt% after the second and fifth runs, respectively (Table 3).

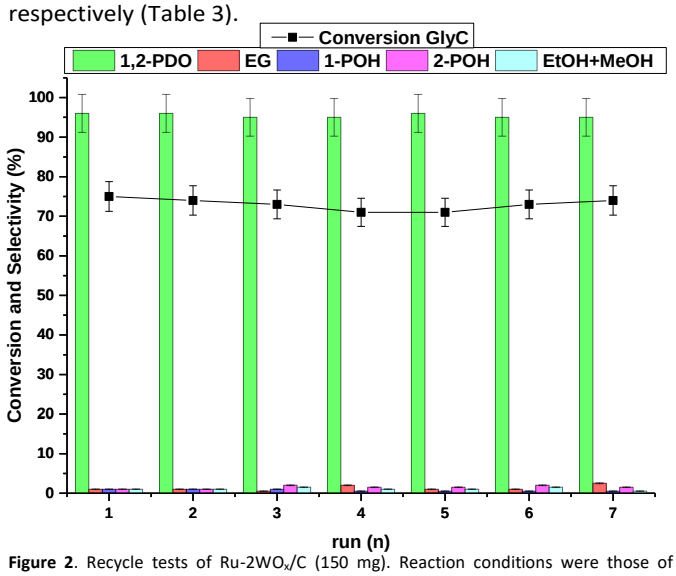

Figure 2. Recycle tests of Ru-$2WO_x$/C (150 mg). Reaction conditions were those of Figures 1, left: aq. glycerol (5 mL, 5 wt%), 150 °C, 5 bar of H_2 bar, 6 h.

Table 3. Leaching of Ru and W after recycles, by ICP analysis

Entry	Run	Ru (wt%)[a]	W (wt%)[a]
1	1	<0.01	4.5%
2	2	<0.01	0.3%
3	5	<0.01	0.1%

[a] Leaching of Ru and W (wt%) was calculated based on the initial loading of both metals. ICP analyses were performed as described in Table 1.

These results were confirmed by additional recycle experiments (carried out under the conditions of Figure 2) where the recovered catalyst was subjected to ICP analyses as described in Table 1. Although leaching of WO_x species was detected, this gradually diminished in the repeated uses and had no effects on the active sites of the catalyst.

A similar behavior was described in previous studies. i) In the hydrogenolysis of 1,4-anhydroerythritol catalyzed by Pt-WO_3/SiO_2 where albeit a W leaching of 3.6, 1.8, and 0.2 wt% observed after the first reaction and two subsequent recycles, no loss of Pt and a stable catalytic activity were reported.[47] ii) In the conversion of cyclopentene to glutaraldehyde catalysed by mesoporous WO_3/SBA-15. In this latter case leaching of WO3 determined a slight decrease of catalyst performance which was offset through thermal regeneration of WO_3/SBA-15 before its reuse.[48] Authors concluded that the presence of polymeric tungsten species or crystalline WO_3 which weakly interacted with the support (during catalyst preparation and use), were responsible for the observed leaching effects. This was consistent with the behaviour of Ru-$2WO_x$/C (Figure 2 and Table 3); such an aspect, however, was not further investigated by us.

A final set of recycle experiments was designed by exposing Ru-$2WO_x$/C to harsher more stressing conditions, specifically by carrying out five subsequent hydrogenolysis reactions at 150 °C, but at a higher pressure (35 bar) and for a longer time (12 h) than those of Figure 2. The catalyst proved stable over

time: a quantitative conversion of glycerol was observed in all repeated tests, while the 1,2-PDO selectivity slightly decreased from 88 % (run 1) to 82% (run 5): this drop was in line with pressure effects described in Figure 1 (details of this study are in the ESI section, Figure S4).

Catalyst characterization: morphological and structural properties. The best performant catalyst for the hydrogenolysis of glycerol, Ru-2WO_x/C, was considered for this study. A fresh and a used sample (before and after the reaction) of Ru-2WO_x/C were characterised by XPS, TEM, and XRD. The "used" specimen was the catalyst recovered after two hydrogenolysis tests carried under the conditions of Figure 1 (150 °C, 5 bar, 6 h). For comparison, XPS analysis was performed also for a sample containing only W, 2WO_x/C (entry 5, Table 1).

XPS analyses. Spectral line binding energies were referred to the C at 284.4 eV. The three investigated samples (fresh and used Ru-2WO_x/C and 2WO_x/C) did not show surface charging during analysis; though, due to the large amount of C with respect to Ru (the C/Ru ratio is around 20), only the Ru3p doublet band was recorded, while the Ru3d band was overlapped by the much more intense C1s band. The standard energy differences between different tungsten oxides and ruthenium species were considered in the curve filling process of the Ru3p and W4f energy region of the investigated systems. The following section summarizes the salient aspects inferred from XPS analysis while spectra have been reported in the ESI section (Figures S5-S7).

In the fresh Ru-2WO_x/C sample, the $W4f_{7/2}$ signal at 35.1 eV was characteristic of WO_3 and matched the literature data.[49] The presence of some W(V) could not be excluded, but the very low amount of W with respect to oxygen in the analysed region prevented any significant fit on the O1s band involving contributions from different W oxides. The $Ru3p_{3/2}$ signal at 462.6 eV was in agreement with the presence of Ru oxide, RuO_2.[50,51] However, the small difference in BE between oxidized and metallic species in the $Ru3p_{3/2}$ band could not rule out the presence of Ru in oxidation states lower than +4.

Notwithstanding the W-leaching (Table 3) observed for the used Ru-2WO_x/C sample, the corresponding XPS spectra did not show significant changes of $W4f_{7/2}$ and $Ru3p_{3/2}$ signals compared to those of the fresh catalyst, except for a slightly smaller FWHM (full width at half maximum) of the $Ru3p_{3/2}$ band. This suggested a preference for a defined chemical/oxidation state of Ru.

In the 2WO_x/C sample, the $W4f_{7/2}$ signal was consistent with the structure of WO_3 and the reduced FWHM suggested a better-defined chemical state of tungsten. This made the presence of W(V) less probable compared the Ru-doped samples, albeit it could not be completely excluded also in this case.[52]

TEM analysis. High-resolution scanning transmission electron microscopy (HRSTEM), high-angle annular dark-field (HAADF)-STEM and EDX analyses were carried out on fresh and used Ru-2WO_x/C.

The EDX mapping analysis of fresh Ru-2WO_x/C indicated a uniform dispersion of both metals (Ru and W) on the surface of the C support (Figure 3A), while TEM images showed the presence of very small Ru-nanoparticles with an average size of 1.5 ± 0.2 nm and 1.6 ± 0.4 nm for both the fresh and the used catalyst, respectively (Figure 3B).

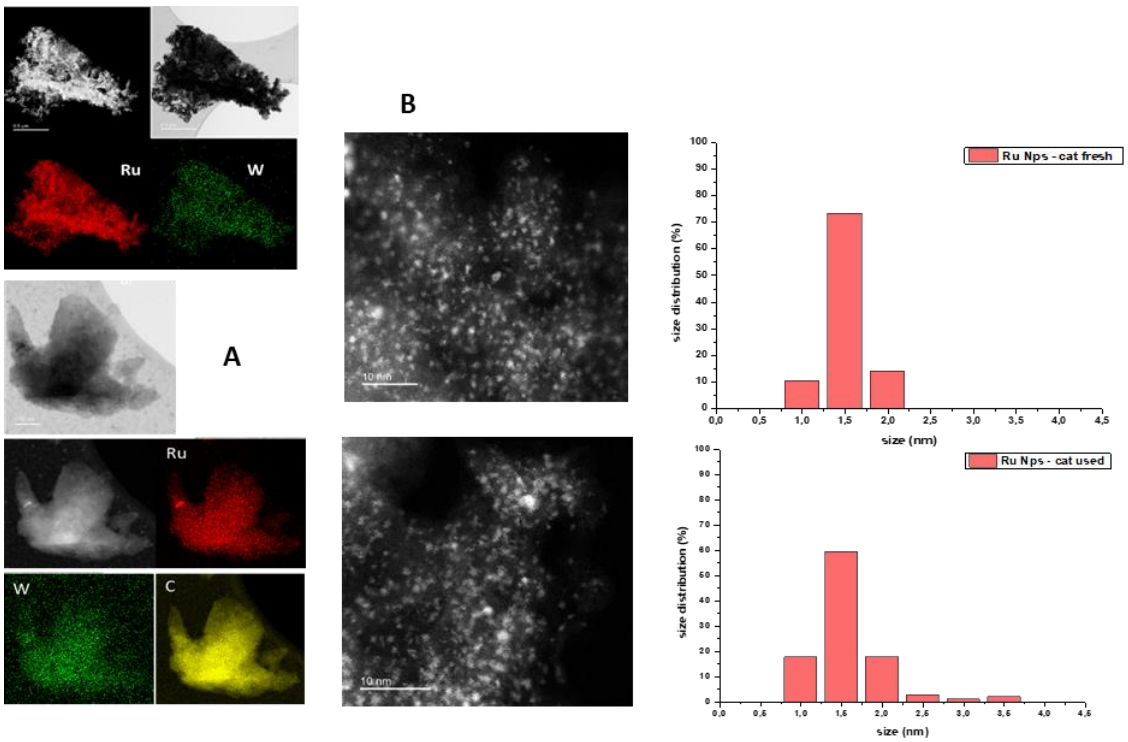

Figure 3. A: EDX mapping analysis of Ru-2WO_x/C. B: STEM images (left) and size distribution of Ru nanoparticles (right) of Ru-2WO_x/C. Top and bottom of Figure 3A and 3B refer to the fresh and the used catalyst. The size of Ru was averaged on more than 100 nanoparticles.

This evidence not only highlighted how the catalyst preparation was effective in achieving a homogeneous distribution of the metal components on the catalyst, but it corroborated the results of recycle tests: the stable performance of Ru-2WO_x/C during its reuses (Figure 2) was consistent with the size preservation of metal (Ru) nanoparticles from the fresh to the used sample. A further indication of the nature and composition of nanoparticles came from the cross-section analyses reported in Figure 4.

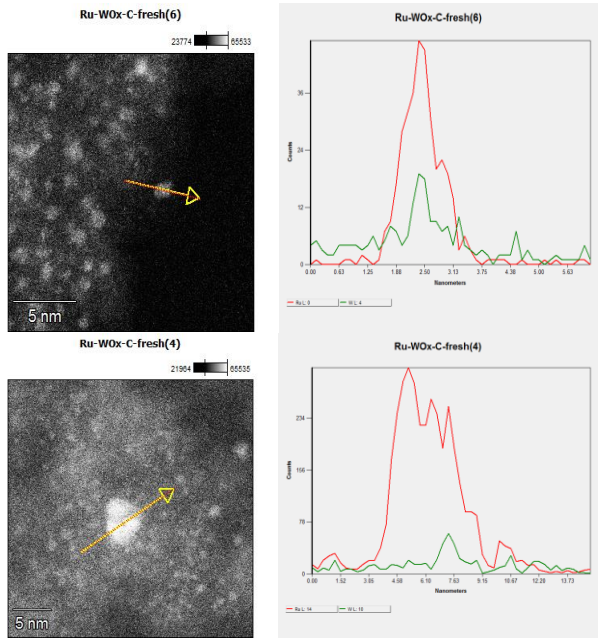

Figure 4. Cross section analysis of nanoparticles in the Ru-2WO_x/C catalyst. Top: a single dot; bottom: an agglomerate present of the catalyst surface

High-resolution images showed the presence of crystalline ordered dots (top) along with single or randomly aggregated dots (bottom) which might be ascribed to WO_x clusters smaller than 100 nm. The close proximity of the two metals indicated that a strong Ru-W interaction was possible although the formation of any bimetallic alloy could not be detected. Moreover, the amount of W in the chosen particles/ agglomerates (top and bottom) was lower than expected for Ru-2WO_x/C (Ru:W=4 mol/mol; compare profiles of Figure 5, left). Recent studies on the activity of a multimetallic Pt-WO_x/ZrO_2 system (Pt-WO_x supported on ZrO_2) for the hydrogenolysis of glycerol demonstrated that the reaction was structurally sensitive to the domain size of surface WOx clusters.[53] WO_x/ZrO_2 was categorised as a superacid solid where medium size clusters (medium polymerized WO_x domains) imparted a strong Brønsted acidity to boost the selective formation of 1,3-PDO, while smaller clusters (isolated WO_x and/or with a low degree of polymerization) behaved as Lewis acid sites. Another investigation described similar acid features for a Pt-WO_x/Al_2O_3 catalyst which were attributed to different WO_x species comprised of monotungstate, polytungstate and crystalline clusters with variable proportions depending on the W loading.[54] In analogy to these results, whichever the structure of WOx, the acidity of the Ru-2WO_x/C catalyst should plausibly favour the dehydration of glycerol during hydrogenolysis (Path 1 in Scheme 1), thereby improving the selectivity towards 1,2-PDO.

XRD analyses. XRD spectra of fresh and used Ru-2WO_x/C did not offer information on either WO_x or Ru species on the catalyst, since diffraction profiles of both samples matched that of the carbon support (Details are in the ESI section. Figure S8).[55] This result was consistent with TEM analyses that showed a homogeneous dispersion of small nanoparticles undetectable by XRD.

Catalyst characterization: surface acidity and Ru dispersion. The acid nature of the catalysts and the dispersion of the metal active for hydrogenolysis (Ru) were investigated by NH_3-temperature-programmed desorption (NH_3-TPD) and CO chemisorption. This study was aimed at comparing the properties of the bimetallic catalysts used in this work, particularly to explore any effect induced by the change of the W content. Tests were carried out as described in the experimental section, starting from samples (60 mg) of Ru-2WO_x/C, Ru-1WO_x/C and Ru-0.5WO_x/C, respectively, where the Ru amount was constant (5wt%) while the W loading was progressively decreased from 2 to 0.5 wt% (compare Table 1). Moreover, to shed light on the role of the surface acidity, additional NH_3-TPD experiments were carried out on the carbon support as such (NORIT SX 1G: C_{fresh}) and after treating it with aq. HCl according to the same procedure used for the catalyst preparation (NORIT SX 1G: $C_{acid\text{-}treated}$; details are in the experimental section)

Figure 5 shows the results of NH_3-TPD measures. The amount of acid sites was calculated from the desorbed NH_3 as reported in Table 4.

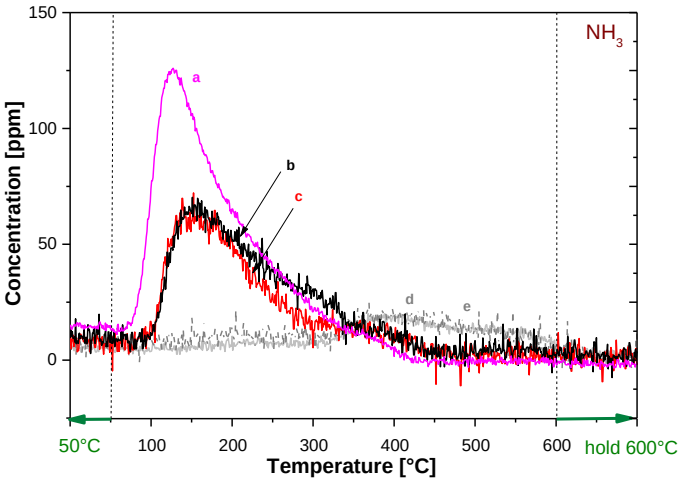

Figure 5. Thermal Programmed Desorption (TPD) up to 600 °C after NH_3 (1000 ppm in He) adsorption at 50 °C for different catalysts: a) Ru2WO_x/C; b) Ru1WO_x/C; c) Ru0.5WO_x/C; d) fresh carbon support; e) acid treated carbon support.

Table 4. Acidity of Ru-WO_x/C catalysts from NH_3-TPD

Entry	Sample	Metal Loading (wt%)		Desorption T (°C)		NH_3 des ($\mu mol/g_{cat}$)
		Ru	W			
1	C_{fresh}[a]	-	-	390	540	26.8
2	$C_{acid\text{-}treated}$[b]			390	Nd[c]	29.8
3	Ru-2WO_x/C	4.8	2.0	127	375	73.3
4	Ru-1WO_x/C	4.7	1.0	155	360	58.8
5	Ru-0-5WO_x/C	4.8	0.5	155	370	46.9

The surface acidity was calculated from desorbed NH_3 in TPD profiles. [a] C_{fresh}: the fresh carbon support (NORIT SX 1G) used in this study. [b] $C_{acid\text{-}treated}$: the carbon support treated under the same acid conditions used for the preparation of Ru-WO_x/C systems.[c] Not determined.

As expected, the fresh and the acid-treated carbon samples displayed some surface acidity which was due to the typical functionalities present on carbon, as carboxylic acids, anhydrides (hydrolysed in aqueous solutions), phenols, and quinones.[26] The corresponding TPD profiles of C_{fresh} and $C_{acid\text{-}treated}$, however, were almost superimposed (curve d and e, respectively: entries 1 and 2), thereby suggesting that even though the acidity of the support could contribute the reaction progress, it (acidity) was not substantially affected by the acid treatment used in the synthesis of Ru-WOx/C samples.[56]

Moving on to the bimetallic samples, the literature correlates the desorption temperature of NH_3 in TPD profiles to the surface acidity, by identifying weak (lower than 300 °C), medium (300-500 °C), and strong (>500 °C) sites.[57] According to this classification, Figure 5 and Table 4 indicated that the three examined catalysts were all characterized by the presence of acid sites of weak-to-medium strength (T desorb in the range of 127-375 °C: entries 2-3), but the total acidity, albeit far higher than that of the support, was considerably different between the samples. Indeed, experiments showed that the lower the W loading, the lower the concentration of acid sites: the amount of desorbed NH_3 progressively decreased from 73.3 to 46.9 $\mu mol/g_{cat}$ as the W content was decreased from 2 to 0.5 wt% (entries 3-5: Ru-2WO_X/C, Ru-1WO_X/C, and Ru-0.5WO_X/, respectively). An additional TPD run – not shown in Figure 5 - on the Ru-2WO_X/C catalyst recovered after its use (same sample of Figure 3, bottom), confirmed a slight drop of surface acidity compared to the fresh system. This behaviour was consistent to the W loss observed during the recycle of the catalyst (Table 3).

CO chemisorption from the gas phase was used to determine the accessible Ru surface area.[58] Table 5 shows the results by reporting the Ru dispersion (D_{Ru}, %).

Table 5. Ru dispersion from CO chemisorption measurements

Entry	Sample	Total CO ads ($\mu mol/g_{cat}$)	D_{Ru} (%)
1	Ru-2WO_x/C	35	7
2	Ru-1WO_x/C	70	14
3	Ru-0-5WO_x/C	77	15

The decreasing of the W loading from 2 to 1 wt% brought about an evident increase of the Ru dispersion from 7 to 14% (entries 1-2). The latter, however, showed only a slight increase to 15% when the W content was further halved to 0.5 wt% (entry 3). This behaviour corroborated the results of TEM experiments: not only Ru and W interacted with each other because of their close proximity on the catalyst surface, but the entity/strength of this interaction was correlated to the W content. Other details of CO chemisorption measures are described in the ESI section (Table S1).

The reaction mechanism. In addition to the above-described Pt-WO_x/ZrO_2 and Pt-WO_x/Al_2O_3 catalysts,[54-55] a significant body of literature on bi- and multi-metallic systems including for example, mesoporous Ti–W oxides,[59] Pt on WO_3/silica-alumina, [60] and Pt-HSiW/SiO_2,[61] led to conclude that WO_x-doping increased the catalyst acidity. In aqueous solutions, especially Brønsted acid sites generated on the WO_x surface, promoted the dehydration of glycerol, while other WO_x species (even slightly reduced W(V)-sites formed in situ by H_2 or glycerol) stabilized adsorption of glycerol and intermediate species during hydrogenolysis. Moreover, the surface acidity of carbon could play a role. This hypothesis was corroborated by several studies, among which two pertinent investigations reported an improved performance of a set of acid-activated Pd/C catalysts in the hydrogenolysis of hydroxymatairesinol (a known lignan) to matairesinol: it was observed that either on carbon or carbon nanofibers, the more acid the support (from 0.0078 to 0.0246 mmol/g of acidity), the more active and selective the catalyst with product yields that increased up to a factor of 4.[62, 63]

These considerations applied also to the WO_x-modified Ru catalysts on C studied here, for which TEM analyses (Figures 3 and 4), NH_3-TPD (Figure 5 and Table 4) CO chemisorption (Table 3) suggested the occurrence of a synergic effect of the two metal components in the form of Ru nanoparticles and (isolated) WO_x acidic clusters. Moreover, the little, but not negligible, acidity of the carbon support (Table 4) could contribute the activation of glycerol over the catalytic surface. The mechanism shown in Figure 6 was therefore hypothesised.

In the first step (A→B), glycerol adsorbs on acid WO_x species, acting either as a H-bond acceptor on Bronsted acid sites (red) and a H-bond donor on Lewis acid sites. The steric hindrance plausibly favours H-bonding of primary hydroxyls with respect to the secondary one. Although not explicitly shown to avoid overburdening Figure 7, similar interactions with acid functions on the C support (see dashed box) are expected to further stabilize glycerol on the catalyst surface. This mode of adsorption has been described for example, in the removal of glycerol from biodiesel washwaters using activated carbon materials.[64]

Thereafter, the moderate (Brønsted) acid strength of surface species is enough to assist dehydration which takes place concurrently to deprotonation and restoration of the catalyst acidity (B→C).

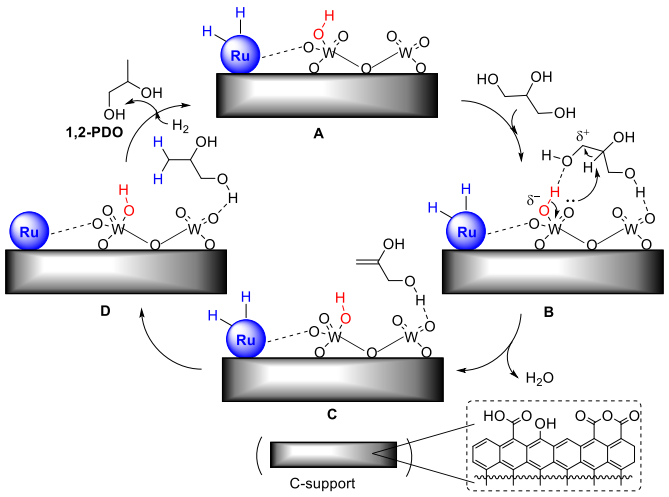

Figure 6. Pictorial view of the hydrogenolysis of glycerol over WOx-modified Ru catalysts on C. The dashed box (bottom): major oxygenated acid species of the support surface.

Prop-2-ene-1,2-diol [$HOCH_2CH(=CH_2)OH$] forms on the catalyst surface (compare path 1, Scheme 1): this species reacts with H atoms deriving from H_2 dissociation on the Ru nanoparticles, producing 1,2-PDO (C→D) which finally desorbs in the aq. solution (D→A). The surface density of acid groups obviously affects the outcome of all steps (rate/selectivity) and it may offer an explanation for the change of the catalyst performance described in Table 2. Particularly, the improved efficiency of the catalysts with the increase of the W loading from 0.5 to 2 wt%, was correlated to the higher concentration of surface WO_x sites which as demonstrated by NH_3-TPD measures. On the other hand, the total inactivity exhibited by WO_x/C (entry 7, Table 2) indicates that the hydrogenolysis reaction becomes successful only on condition that Ru, WO_x and the carbon support act synergistically. It should also be noted that at 150-200 °C, some acid-activated carbons have been reported to catalyse the dehydration of primary alcohols (ROH: R=*n*-Pr, *n*-Bu):[65] these systems however, display a surface acidity far higher (up to 1800 μmol/g) than Ru-WO_x/C samples.

The mechanism of Figure 6 cannot rule out that also secondary hydroxyl groups of glycerol are H-bonded to acid sites (both WO_x and oxygenated species on C) as reported for W-doped Pt-catalysts.[53] However, the mild acidity of Ru-WO_x/C systems hinder the dehydration of sec-OH since in our case the product expected from this reaction (1,3-PDO) has never been detected.

An additional aspect is the presence of Na traces in the catalytic samples. Although it is well known that the doping by alkali metals affect the hydrogenation performance of Ru-based catalysts,[66] it seems unlikely that a similar effect favours the hydrogenolysis of glycerol towards 1,2-PDO in the case of the bimetallic systems investigated here. Indeed, the latter (Ru-WO_x/C) have a Na content (<0.1 wt%) equal to that of the commercial 5% Ru/C which in no way is a selective catalyst.

A brief comment is finally addressed to the metal dispersion (Table 5). Although the investigation of the decrease of the Ru dispersion with the increase of the WO_x content is beyond the scope of the present paper, the best performance of the least dispersed catalyst might suggest that the overall reaction is structure-sensitive.

Experimental

General. Glycerol, 5% Ru/C, $RuCl_3 \cdot H_2O$, Na_2WO_4, aq. HCl (37 wt%), HNO_3 (70 wt%), H_2O_2 (30 wt%), 1,2-propanediol (1,2-PDO), 1-PrOH, 2-PrOH, ethylene glycol (EG), EtOH, MeOH, triglyme, and carbon NORIT SX 1G were commercially available compounds sourced by Aldrich. If not otherwise specified, they were employed without further purification. Water was milli-Q grade. H_2 was from SIAD, Italy.

Catalyst preparation. WO_x-modified Ru catalysts were prepared by a co-impregnation method using $RuCl_3 \cdot H_2O$ and Na_2WO_4 as precursors. Finely powdered carbon (1 g, NORIT SX 1G) was suspended and stirred in milli-Q water (50 mL). In a separate flask, $RuCl_3 \cdot H_2O$ (0.1 g) and Na_2WO_4 (0.128 - 0.09 mg; Ru:W = 1 - 16 mol:mol) were dissolved in milli-Q water (50 mL). The aq. solution of metal precursors was added to the carbon suspension and the resulting mixture was stirred overnight at rt. It was then heated at 80 °C, added with aq. HCl (1 mL; 15 wt%), and kept at 80 °C for 3 h. Thereafter, water was slowly evaporated at 95 °C. The black powder was collected, dried at 180 °C overnight, and reduced at 300 °C in H_2 atmosphere (25 mL/min) for 3 h, and cooled to rt under N_2 (25 mL/min) for 30 minutes. The sample was then washed with milli-Q water (50 mL) and dried under vacuum (5 mbar) at 70 °C for 12 hours before any use.

Catalyst characterisation. Once prepared, Ru-WO_x/C systems were characterized by ICP, XPS, TEM, XRD, and NH_3-TPD.

ICP-MS analyses were performed using a Perkin Elmer Optima 5300DV. Analyses of the fresh and used (post-reaction) catalysts (Tables 1 and 3) were performed after digestion in the presence of a highly oxidant solution under MW irradiation. Details of the digestion procedure and the analytical protocol for ICP measures are reported in the ESI section.

High-resolution scanning transmission electron microscopy (HRSTEM), high-angle annular dark-field (HAADF)-STEM and EDX analyses were recorded on a Hitachi HD-2700 STEM instrument and a JEM-ARM 200F STEM instrument both operated at 200 kV. The samples for TEM were prepared by directly dispersing the fine powders of the products onto a micro-grid carbon polymer supported on a copper grid.

X-ray powder diffraction (XRD) patterns of the catalysts were recorded using a Philips X'Pert powder diffractometer (Bragg–Brentano parafocusing geometry). Nickel-filtered CuKa1 radiation (λ=0.15406 nm) and a voltage of 40 kV were employed.

X-ray photoelectron spectroscopy (XPS) was performed on a Perkin Elmer Φ 5600ci spectrometer using nonmonochromatic Al Kα radiation (1486.6 eV) in the 10−7 Pa pressure range (other details are in the ESI section).

NH_3-temperature-programmed desorption (TPD) was performed using a powdered sample of the catalyst (60 mg) which was sieved at 70-100 µm (140-200 mesh) and then loaded in a quartz microreactor with an internal diameter of 8 mm. The outlet of the reactor was directly connected to a UV-analyzer specific for NH_3 analysis (Limas 11HW, ABB). The sample was pre-treated under He flow at a flow rate of 60 Ncm^3/min in the microreactor at 300 °C for 1 h. Then, the catalyst was cooled down to 50 °C and at this temperature, NH_3 (1000 ppm) was stepwise added to the gas mixture for 30 minutes (reaching the steady-state). NH_3 supply was closed and it was purged in He until the baseline was stable. Finally, the catalyst was heated under temperature programming (TPD) up to 600 °C (heating rate 10 °C/min).

CO chemisorption experiments were carried out on a powdered sample of the catalyst (60 mg). A first CO adsorption isotherm (@ 40°C) was achieved to measure the total amount of adsorbed carbon monoxide (chemisorbed and physisorbed). The catalyst was then outgassed, and a second CO adsorption isotherm was measured to evaluate the amount of physisorbed CO. The total amount of chemisorbed CO was obtained by subtracting the second isotherm from the first one. It should be noted that before the adsorption isotherm measurements, the sample surface was exposed to H_2 atmosphere (4% v/v) for 0.5 h at 500 °C and 1 h at the same temperature in He so as to reduce the surface metal oxide possibly formed during the catalyst storage under air. From chemisorption measurements, the proportion of accessible metal located at the surface of the Ru particles, *i.e.* the dispersion D_{Ru} was calculated from the following expression:

$$D_{Ru} = \frac{mol_{CO}}{mol_{Ru}} * \chi_{Ru-CO} * 100$$

where mol_{CO} was the amount of CO adsorbed on surface Ru atoms and mol_{Ru} was the amount of Ru present in the catalyst. X_{Ru-CO} represented the mean chemisorption stoichiometry, i.e. the average number of Ru atoms on which one CO molecule was adsorbed. In the present study, X_{Ru-CO} was chosen equal to 1.

Acid-treated carbon ($C_{acid\text{-}treated}$: Table 4). Finely powdered carbon (300 mg, NORIT SX 1G) was suspended and stirred in milli-Q water (15 mL). The aq. suspension and the resulting mixture was stirred overnight at rt. It was then heated at 80 °C, added with aq. HCl (0.3 mL; 15 wt%), and kept at 80 °C for 3 h. Thereafter, water was slowly evaporated at 95 °C. The black powder was collected, dried at 180 °C overnight, and reduced at 300 °C in H2 atmosphere (25 mL/min) for 3 h, and cooled to rt under N2 (25 mL/min) for 30 minutes. The sample was then washed with milli-Q water (50 mL) and dried under vacuum (5 mbar) at 70 °C for 12 hours before any use.

Reaction procedure. In a typical hydrogenolysis experiment, a 25-mL tubular reactor of borosilicate glass (Pyrex) was charged with 5 mL of a 5% w/w glycerol water solution, and the catalyst of choice (150 mg, selected among those reported in Table 2). The vessel was placed in a jacketed steel autoclave equipped with a manometer and two needle valves by which, at rt, H_2 was admitted at the desired pressure. The autoclave was then heated by oil circulation at the desired temperature (120-170 °C), while the mixture was kept under magnetic stirring at a rate of 1300 rpm. After 6-12 hours, the autoclave was cooled to rt, and purged. An aliquot (0.5 mL) of the water solution was collected, mixed with an aq. solution of triethylenglycol dimethylether as external standard [triglyme, $MeO(CH_2CH_2O)_3Me$; 0.01 M, 0.5 mL], and analysed by GC and GC/MS to determine the conversion of glycerol and the selectivity towards liquid products (Table 2), and confirm their structure.

GC–MS (EI, 70 eV) and GC/FID analyses were performed with an HP5-MS capillary column (L = 30 m, Ø = 0.32 mm, film = 0.25 mm) and an Elite-624 capillary column (L = 30 m, Ø = 0.32 mm, film =1.8 mm), respectively.

GC calibration curves for the reactant (glycerol) and the major liquid products (EG, 1,2-PDO, 2-PrOH, and EtOH) are reported in the ESI section (Figures S9-S13). Gaseous by-products were collected after the reaction catalysed by Ru/C was complete (Figure S1): an aliquot (ca 2 L) of the gaseous mixture vented from the autoclave was conveyed to a rubber reservoir and analysed by GC/MS. This confirmed the formation of CO, CH_4, and propane.

The same reaction procedure was repeated by changing the glycerol concentration from 5 wt% to 7.5, 10, 15 and 20 wt% (150 °C, 5 bar, 12 h: Figure S3).

Conclusions

The potential of new bimetallic Ru-WO_x/C catalysts has been explored for the selective synthesis of 1,2-PDO by the hydrogenolysis of glycerol in aqueous solutions. Among salient aspects of this study, it has been demonstrated that: i) glycerol conversion substantially improves up to 100% by reducing the Ru:W molar ratio up to 4:1 mol/mol. Further reduction of this ratio is impracticable as it leads to catalyst reproducibility issues at W-loadings > 2 wt%; ii) albeit WO_x (supported on C) is totally ineffective for the reaction, W-doping of Ru-based systems is crucial to boost the reaction selectivity up to 97-98%. By contrast, Ru/C alone favors multiple C-C bond cleavage side-reactions yielding ethylene glycol as the major product in the liquid phase along with a large amount of gaseous derivatives (carbon loss of 51%); iii) Ru-WO_x/C catalysts can be recycled without any loss of activity and selectivity. Leaching of W occurs in the aqueous solution, but it diminishes and stabilizes after few repeated runs, and most of all, it is uninfluential on the catalyst performance.

Overall, the here described protocol offers conversion and selectivity equally efficient to those of the best existing methods for the synthesis of 1,2-PDO from glycerol (based on Ru/Cu-based systems), with the advantage of requiring far milder reaction conditions (150 °C and 5 bar *vs* 180-230 °C and 80-100 bar). The result is consistent with the complementary information offered by STEM and TPD characterization techniques on Ru and WO_X components of the bimetallic system. This leads to hypothesize a synergic effect between the two metals in the form of Ru nanoparticles uniformly dispersed on the carbon support and in close proximity to

different WO_x species whose structure, although not conclusively defined, may include monotungstate, polytungstate and crystalline clusters. The proposed mechanism takes into account the acid character (both of Brønsted and Lewis type) of the WO_x sites which allows for the adsorption via H-bonding and dehydration of glycerol to prop-2-ene-1,2-diol (PED), while Ru is responsible for the hydrogenation of PED to 1,2-PDO via hydrogen spillover onto the surface. The total sequence is positively affected by the concentration of acid sites which increases with the W-loading. However, in analogy to the behavior reported for other W-based catalysts, a high metal loading (> 2wt%) brings about the formation of tungsten species loosely adsorbed on the support that may cause leaching and adverse effects on the catalyst preparation.

Author Contributions

Alessandro Bellè: Conceptualization, Investigation, Methodology, Writing-Original draft preparation; Kohei Kusada: Investigation, Methodology; Hiroshi Kitagawa: Supervision, Validation; Alvise Perosa: Writing-Reviewing, Funding acquisition. Validation; Maurizio Selva: Conceptualization, Supervision, Writing-Reviewing and Editing, Funding acquisition; Daniele Polidoro: Investigation; Lidia Castoldi: Investigation, Methodology, Writing draft preparation.

Conflicts of interest

There are no conflicts to declare.

Acknowledgements

Dr. K. Kusada gratefully acknowledges Ca' Foscari University for granting a visiting scholarship for his stay in Venezia (June-August 2019; public grant n. 777/2018, profile 11J). Dr. T. Tabanelli at the University of Bologna, Prof. L. Castoldi at the Polytechnic University of Milano, Prof. E. Cattaruzza and Mr. D. Polidoro at Ca' Foscari University are gratefully acknowledged for their help in the synthesis and characterization of some catalysts.

References

1. R. Christoph, B. Schmidt, U. Steinberner, W. Dilla, R. Karinen, *Glycerol. Ullmann's Encyclopedia of Industrial Chemistry*, 2012, **17**, 67-82
2. J. Kaur, A. K. Sarma, M. K. Jha, P. Gera *Biotech. Reports* 2020, **27**, e00487.
3. M. K. Aroua, P. Cognet *Front. Chem*. 2020, **8**, 69.
4. G. N. Oliveira, C. Barbosa, F. C. Araújo, P. H. G. Souza, A. V. H. Soares, F. C. Peixoto, J. W. M. Carneiro, F. B. Passos In Jatropha, Challenges for a New Energy Crop (Eds.: S. Mulpuri, N. Carels, B. Bahadur), Springer, Singapore, **2019**, pp. 383-414
5. A. D. da Silva Ruy, R. M. de Brito Alves, T. L. R. Hewer, D. de Aguiar Pontes, L. Sena Gomes Teixeira, L. A. Magalhães Pontes *Catal. Today* 2020, in the press., doi: 10.1016/j.cattod.2020.06.035
6. H. Zhao, L. Zheng, X. Li, P. Chen, Z. Hou *Catal. Today* 2019, **355**, 84-95
7. Y. Wang, J. Zhou, X. Guo *RSC Adv*., 2015, **5**, 74611–74628.
8. D. Sun, Y. Yamada, S. Sato, W. Ueda *Appl. Catal. B: Environ*. 2016, **193**, 75–92.
9. M. A. Dasari, P.-P. Kiatsimkul, W. R. Sutterlin and G. J. Suppes, *Appl. Catal., A*, 2005, **281**, 225-231.
10. A. Perosa, P. Tundo *Ind. Eng. Chem. Res*. 2005, **44**, 8535-853
11. B. K. Kwak, D. S. Park, Y. S. Yun and J. Yi, *Catal. Commun*., 2012, **24**, 90-95
12. S. H. Zhu, X. Q. Gao, Y. L. Zhu, Y. F. Zhu, H. Y. Zheng and Y. W. Li, *J. Catal.,* 2013, **303**, 70-79
13. Y. Du, C. Wang, H. Jiang, C. Chen, R. Chen, *Ind. Eng. Chem*. 2016, **35**, 62–267.
14. N. N. Pandhare, S. M. Pudi, P. Biswas, S. Sinha *Org. Process Res. Dev*. 2016, **20**, 1059-1067
15. P. Kumar, A. K. Shah, J.-H. Lee, Y. H. Park, U. Stangar *Ind. Eng. Chem. Res*. 2020, **59**, 6506-6516
16. Z. L. Yuan, P. Wu, J. Gao, X. Y. Lu, Z. Y. Hou and X. M. Zheng, *Catal. Lett.*, 2009, **130**, 261-265
17. X. Zhang, G. Cui, M. Wei *Ind. Eng. Chem. Res*. 2020, **59**, 12999-13006
18. J. Liu, L. Ruan, J. Liao, A. Pei, K. Yang, L. Zhu, B. Hui Chen *New J. Chem.*, 2020, **44**, 16054-16061
19. R. B. Mane, S. T. Patil, H. Gurav, S. S. Rayalu, C. V. Rode *ChemistrySelect* 2017, **2**, 1734–1745
20. R. Mane, S. Patil, M. Shirai, S. Rayalu, C. Rode *Appl Catal B: Environ* 2017, **204**, 134–146
21. T. Miyazawa, S. Koso, K. Kunimori and K. Tomishige, *Appl. Catal., A*, 2007, **329**, 30-35
22. J. Feng, W. Xiong, B. Xu, W. D. Jiang, J. B. Wang and H. Chen, *Catal. Commun.*, 2014, **46**, 98-102
23. A. V. H. Soares, J. B. Salazar, D. D. Falcone, F. A. Vasconcellos, R. J. Davis, F. B. Passos *J. Mol Catal A: Chem* 2016, **415**, 27–36
24. T. Jiang, Y. X. Zhou, S. G. Liang, H. Z. Liu and B. X. Han *Green Chem*., 2009, **11**, 1000-1006.
25. H. Liu, S. Liang, T. Jiang, B. Han, Y. Zhou *Clean – Soil, Air, Water* 2012, **40**, 318–324
26. A. Bellè, T. Tabanelli, G. Fiorani, A. Perosa, F. Cavani, M. Selva *ChemSusChem* 2019, **12**, 3343–3354,
27. W. Zhou, J. Luo, Y. Wang, J. Liu, Y. Zhao, S. Wang, X. Ma *Appl. Catal B: Environ* 2019, **242**, 410–421
28. L. Liu, T. Asano, Y. Nakagawa, M. Tamura, K. Okumura, K. Tomishige *ACS Catal*. 2019, **9**, 10913-10930
29. Y. Liu, C. Luo, H. Liu *Angew. Chem*. 2012, **124**, 3303–3307
30. L. Wei, R. Bibi, W. Tian, L. Chen, Y. Zheng, N. Li, J. Zhou *New J. Chem*., 2018, **42**, 3633--3641
31. C. Li, G. Xu, X. Zhang, Y. Fu Chin. *J. Chem*. 2020, **38**, 453－457
32. M. Yabushita, N. Shibayama, K. Nakajima, A. Fukuoka *ACS Catal*. 2019, **9**, 2101-2109
33. M. Pagliaro, M. Rossi In The Future of Glycerol, New Uses of a Versatile Raw Material, (Eds. J. H Clark, G. A Kraus), RSC Green Chemistry Book Series, 2010
34. S. Fulignati, C. Antonetti, D. Licursi, M. Pieraccioni, E. Wilbersb, H. J. Heeresb, A.M. Raspolli Galletti, *Appl. Catal. A*, 2019, **578**, 122–133
35. C. Rajkumar, B. Thirumalraj, S. M. Chen, P. Veerakumar, S.-B. Liu, *ACS Appl. Mater. Interfaces* 2017, **9**, 31794–31805.
36. A. S. Aricò, Z. Poltarzewski, H. Kim, A. Morana, N. Giordano, V. Antonucci *J. Power Sources* 1995, **55**, 159–166.
37. W. Zang, G. Li, L. Wang, X. Zhang, *Catal Sci Technol* 2015, **5**, 2532–2553
38. A. M. Robinson, J. E. Hensley, J. Will Medlin, *ACS Catal* 2016, **6**, 5026–5043
39. M. Balaraju, V. Rekha, P.S. Sai Prasad, B.L.A. Prabhavathi Devi, R.B.N. Prasad , N. Lingaiah *Appl. Catal. A Gen*. 2009, **354**, 82–87.
40. A. Alhanash, E. F. Kozhevnikova, I. V. Kozhevnikov *Catal. Lett* 2008, **120**, 307–311.
41. D. G. Barton, S. L. Soled, G. D. Meitzner, G. A. Fuentes, E. Iglesia. *J. Catal*. 1999, **181**, 57–72
42. V. I. Baranenko, V. S. Kirov, *Sov. At. Energy* 1989, **66**, 30–34.
43. H. A. Pray, C. E. Schweickert, B. H. Minnich *Ind. Eng. Chem*. 1952, **44**, 1146–1151.

44. L. Ma, D. He, Z. Li, *Catal. Commun*. 2008, **9**, 2489–2495.
45. L. Guo, J. Zhou, J. Mao, X. Guo, S. Zhang, *Appl. Catal. A Gen*. **2009**, *367*, 93–98.
46. F. K. Kazi, A. D. Patel, J. C. Serrano-Ruiz, J. A. Dumesic, R. P. Anex, *Chem. Eng. J*. 2011, **169**, 329–338
47. L. Liu, T. Asano, Y. Nakagawa, M. Tamura, K. Tomishige *Green Chem*. 2020, **22**, 2375–2380.
48. X.-L. Yang, R. Gao, W.-L. Dai, K. Fan *J. Phys. Chem. C* 2008, **112**, 3819-3826
49. N. Tammanoon, T. Iwamoto, T. Ueda, T. Hyodo, A. Wisitsoraat, C. Liewhiran, Y. Shimizu *ACS Appl Mater Interfaces* 2020, **12**, 41728-41739.
50. K. Qadir, S. H. Joo, B. S. Mun, D. R. Butcher, J. Russell Renzas, F. Aksoy, Z. Liu, G. A. Somorjai, J. Y. Park *Nano Lett*. 2012, **12**, 5761–5768.
51. W. Wang, Y. Li, H, Wang *React. Kinet. Mech. Catal*. 2013, **108**, 433–441
52. Z. Cui, L. Feng, C. Liu, W. Xing, *J. Power Sources* 2011, **196**, 2621–2626
53. W. Zhou, J. Luo, Y. Wang, J. Liu, Y. Zhao, S. Wang, X. Ma *Appl. Catal. B Environ.* 2019, **242**, 410–421.
54. S. Zhu, X. Gao, Y. Zhu, Y. Li *J. Mol Catal A: Chem* 2015, **398**, 391–398
55. X-Y. Liu, M. Huang, H.-L. Ma, Z.-Q. Zhang, J.-M. Gao, Y.-L. Zhu, X.-J. Han, X.-Y. Guo *Molecules* 2010, **15**, 7188-7196
56 Authors wish to thank a referee for having prompted further investigations on the acidity of the carbon support.
57 H. Atia, U. Armbruster, A. Martin, *J. Catal*. 2008, **258**, 71-82.
58 F. Micoud, F. Maillard, A. Bonnefont, N. Job, M. *Chatenet Phys. Chem. Chem. Phys*., **2010**, *12*, 1182–1193
59. Y. Zhang, X.-C. Zhao, Y. Wang, L. Zhou, J. Zhang, J. Wang, A. Wanga, T. Zhang *J. Mater. Chem. A*, 2013, ***1***, 3724–3732
60. S. Feng, B. Zhao, L. Liu, J. Dong *Ind. Eng. Chem. Res*. 2017, **56**, 11065-11074
61. S. Zhu, Y. Zhu, S. Hao, L. Chen, B. Zhang, Y. Li *Catal Lett* 2012, **142**, 267–274
62 H. Markus, P. Maki-Arvela, N. Kumar, N. V. Kulkova, P. Eklund, R. Sjoholm, B. Holmbom, T. Salmi, D. Yu. Murzin *Catal Lett* 2005, **103**, 125-131
63 H. Markus, A. J. Plomp, P. Maki-Arvela, J. H. Bitter, D. Yu. Murzin, *Catal Lett* 2007, **113**, 141-146S.
64 S. Liua, S. Reddy Musukua, S. Adhikarib, S. Fernando *Environ Technol* 2009, **30**, 505–510
65 (a) J. Bedia, J. M. Rosas, J. Marquez, J. Rodrıguez-Mirasol, T. Cordero *Carbon* 2009, **47**, 286–294; (b) G. Szymajski, G. Rychlicki *Carbon* 1991, 29, 489-498.
66 Cao, J. R. Monnier, J. R. Regalbuto *J. Catal.* 2017, *347*, 72–78